Journal of Japan Association for Earthquake Engineering, Vol. 21, No. 3, 2021

PROPOSAL OF EMPIRICAL EQUATION ON PHASE TRANSFORM ANGLE OF SANDY SOILS

Takeko MIKAMI[1] and Nozomu YOSHIDA[2]

[1] Team Leader, Engineering Department, Kiso-Jiban Consultants Co., Ltd.,
Chiba, Japan, mikami.takeko@kiso.co.jp
[2] Member, Institute member, Disaster Mitigation Institute, Kanto Gakuin University,
Yokohama, Japan, nyoshida@kanto-gakuin.ac.jp

ABSTRACT: A phase transform angle is known to be an important parameter in the liquefaction analysis, but there is little research on the phase transform angle, it is assumed to be constant or to be proportional to the internal friction angle in practical. In this study, we read off phase transform angles and the internal friction angles from the cyclic shear test results on sand under the triaxial condition. It is found that the phase transform angles scatter between 18 and 28 degrees, and there is strong correlation with the internal friction angle when the fines content is less than 20 %. Based on the findings, an empirical equation is proposed in which the phase transform angle is expressed as a function with respect to the internal friction angle.

Keywords: Phase transform angle, Empirical equation, Sandy soil, Stress path

1. INTRODUCTION

Phase transform is a phenomenon at which dilatancy characteristics change from contraction to expansion. Since the stress state at the phase transform lies on the linear line passing the origin as called the phase transform line[1), 2)] in the effective stress-shear stress diagram (effective stress path diagram, hereafter), it is characterized by the slope angle of the line which is called a phase transform angle. Because of its nature, it is one of the key parameters controlling the dilatancy behavior during earthquake, but it has not been paid much attention in the engineering practice because of the two reasons.

One reason is that it is a troublesome job to read a phase transform angle from the effective stress path diagram directly. Since the effective stress path diagram is not required as the output of the cyclic undrained triaxial test for liquefaction strength (JGS 0541-2009)[3)] (standard method in Japan defined by the Japanese Geotechnical Society), it is not included in the report of the liquefaction strength test. One needs to obtain the digitized test data, draw the stress-path diagram, and read off the phase transform angle. As described later, phase transform angles read off by engineer scatter significantly. Therefore, it is hardly utilized in the practice. The other reason is the practical method to evaluate parameters of

constitutive models in liquefaction analysis. The parameters are usually determined so that liquefaction strength agrees with test result. Therefore, the phase transform angle is not interested.

There is nearly no research on the phase transform angle possibly because of the above two reasons. Thus, there is no empirical research on the phase transform angle. In practice, it is expressed as a function with the internal friction angle[4] or it is assumed to be a constant value[5] regardless of material characteristics such as density and fines content, etc. It looks that the phase transform angle is determined much easier compared with other parameters such as the internal friction angle in the liquefaction analysis.

Nagumo et al.[6] investigated the effect of the phase transform angle in the analysis of a sheet pile type quay wall by using a computer program FLIP ROSE[7], in which a multiple spring model is used as stress-strain relationships[8]. They compared two cases; the one uses 20 degrees and the other 28 degrees for the phase transform angles. Here, they evaluated parameters related to liquefaction characteristics other than the phase transform angles so that the liquefaction strength curve and hysteretic behaviors agree with test result. They found that there are significant differences in the displacement, the deformed shape, and the subsidence although the liquefaction strength curves are almost identical. There is about two times difference in the vertical displacements at the ground behind the quay wall. They also reported that the subsidence continues during the excess porewater pressure dissipation process when the phase transform angle is 28 degrees, whereas the ground begins to uplift, which results in smaller subsidence, when the phase transform angle is 20 degrees. In the same report, they also discussed human error in reading the phase transform angle. Here, eight engineers read off the phase transform angle using the same test data, but the angles scatter between 12 and 27 degrees; the standard deviation was 3 degrees. This research showed the importance to use the relevant phase transform angle and the difficulty to evaluate it.

In the liquefaction analysis, it is suggested to read off the phase transform angle from the test data, but, as described before, it is a troublesome work and there is large human error. Then, we collect liquefaction strength test data and read off the phase transform angle and the internal friction angle carefully, and discuss the nature of them. Finally we propose an empirical equation to evaluate the phase transform angle.

2. TEST METHOD AND RESULTS

Liquefaction strength test data on Toyoura sand and undisturbed soil samples taken from natural ground[9], which are simply called "undisturbed samples" hereafter, are used in this research. Toyoura sand with particle density ρ = 1.640 g/cm^3, and minimum and maximum density ρ_{dmin} = 1.341 g/cm^3 and ρ_{dmax} = 1.639 g/cm^3, respectively, are compacted following the JGS standard[10] so that relative densities D_r = 30, 40, 50, and 80 %, and are tested. On the other hand, undisturbed samples are gathered at five sites in the port areas by means of tube sampling and are trimmed with 5 cm diameter and 10 cm height. Material data of the undisturbed samples are shown in Table 1. There are several data whose fines content F_c is greater than 35 %. Silty sand with large fines content is sometimes considered to be not liquefiable in the design specifications, but the sandy soil used in this study is non-plastic. Therefore, it is to be considered as liquefiable soil. Conversion N value, N_1, is evaluated based on the design specification of highway bridge[11],

$$N_1 = 170N/(\sigma'_v + 70) \quad (\sigma'_v \text{ in kPa}) \tag{1}$$

Liquefaction strength tests are carried out based on JGS 0541-2009. The initial effective confining stress σ'_c is 100 kPa for the Toyoura sand and those for the undisturbed soils are set to be the same as the effective overburden stresses. Sinusoidal waves are applied with loading speed 0.1 Hz for the Toyoura sand and 0.5 Hz for the undisturbed samples by a triaxial test apparatus. The cyclic loading is continued up to double amplitude axial strain DA = 10 %.

3. EVALUATION OF PHASE TRANSFORM ANGLE

Effective stress path diagram is drawn for each specimen at first, then a phase transform point, a point at which the effective stress increment changes from negative to positive is read off. The phase transform angle is calculated as the slope angle of the line connecting the origin and the phase transform point. An example is shown in Fig. 1; (a) is the effective stress path diagram and (b) shows the change of the excess porewater pressure. The red solid and the blue dashed lines are the Mohr–Coulomb failure line and a phase transform line, respectively. Red circles are phase transform points. Blue circles in Fig. 1(b) correspond to the red circles in Fig. 1(a). Phase transform points are read off in the region where the excess porewater pressure ratio $\Delta u/\sigma'_c$ exceeds about 0.5. Excess porewater pressures at the phase transform are maximal in each cycle after the cyclic mobility behavior becomes clear. The human error can be made small when noticing these characteristics.

4. PHASE TRANSFORM AND MATERIAL CHARACTERISTICS

Table 1 Material data

Specimen name		Sampled depth (m)	Overburden stress σ'_v (kPa)	SPT-N value	Conversion N value, N_1	Wet density ρ_t (g/cm^3)	Moisture content w (%)	Fines content F_c (%)	Clay content P_c (%)	Plasticity index I_P
Site A	A-01	3.4 – 4.4	34	17	27.5	1.822	29.5	18	5	—
	A-02	6.4 – 7.3	51	17	23.7	1.866	30.1	20	6	—
	A-03	9.9 – 10.7	72	8	9.5	1.898	28.6	51	10	—
	A-04	1.7 – 2.5	34	15	24.3	1.879	24.0	21	5	—
	A-05	4.7 – 5.4	35	28	44.9	1.804	21.1	9	2	—
	A-06	8.7 – 9.5	60	22	28.5	1.890	28.4	17	3	—
Site B	B-07	9.8 – 10.9	59	7	9.2	1.969	26.1	54	11	—
	B-08	11.5 – 12.0	65	7	8.8	2.073	19.4	15	4	—
	B-09	13.3 – 14.0	74	7	8.2	1.884	32.7	44	13	—
	B-10	15.0 – 15.8	81	13	14.4	1.874	31.9	21	4	—
Site C	C-11	10.8 – 11.8	128	15	12.7	1.820	24.6	19	4	—
	C-12	2.0 – 3.0	75	10	11.6	1.895	23.1	13	4	—
	C-13	11.6 – 12.6	144	15	11.8	1.890	30.8	24	6	—
Site D	D-14	10.7 – 11.7	133	20	16.5	1.843	28.1	26	6	—
	D-15	14.2 – 15.4	158	14	9.9	1.836	37.9	62	12	14.4
	D-16	18.6 – 20.1	188	6	3.9	1.821	38.5	62	16	15.2
Site E	E-17	6.5 – 7.5	89	13	13.7	1.851	18.7	26	5	—
	E-18	10.0 – 11.0	117	8	7.2	1.968	26.5	47	10	—

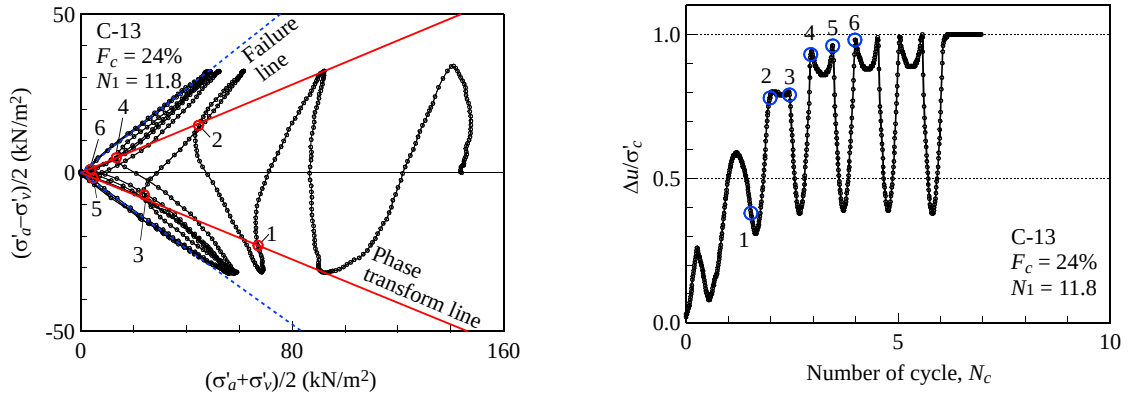

(a) Effective stress path (b) Excess porewater pressure vs. number of cycles

Fig. 1 Example of test result (undisturbed sample C-13)

Three effective stress path diagrams of the Toyoura sand with relative density D_r = 30 %, 50 %, and 80 % are compared in Fig. 2 to see the effect of density on the phase transform angle. The coordinate axes are set identical so as to make the comparison easy. It is clearly seen that the shear stress of the phase transform point becomes small as the relative density becomes small, and it becomes large as the relative density becomes large.

In order to see the effect of grain size on the phase transform angle, effective stress path diagrams of the undisturbed samples are compared in Fig. 3. The curves seem to become rounder near the origin as the fines content becomes large, which makes evaluation of the phase transform angle more difficult. In the case of Fig. 3(c) (E-18 with fines content F_c = 47 %), for example, the phase transform angle cannot be decided; the phase transform points in the compression side lie almost on a horizontal line and there is no phase transform point in the elongation side. There are several cases that the phase transform angle was difficult to determine same as this case and they are not included in this research.

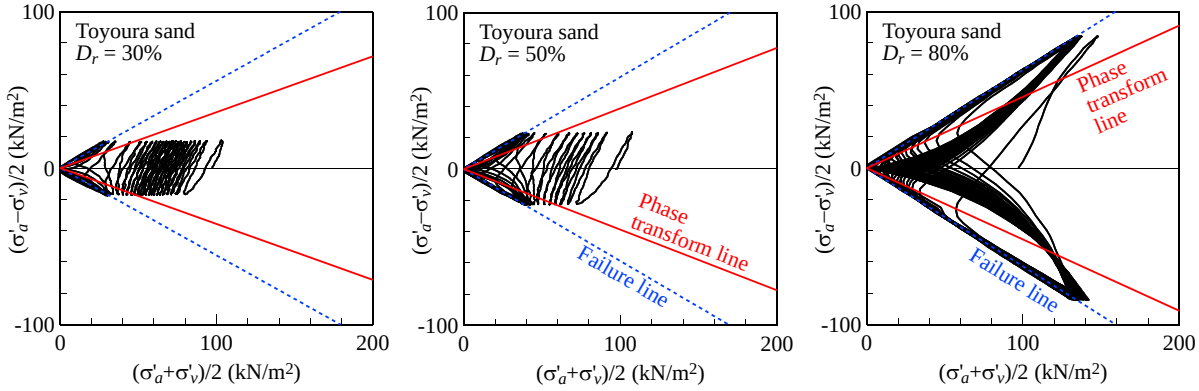

(a) D_r = 30 % (b) D_r = 50 % (c) D_r = 80 %

Fig. 2 Effective stress path diagram of Toyoura sand

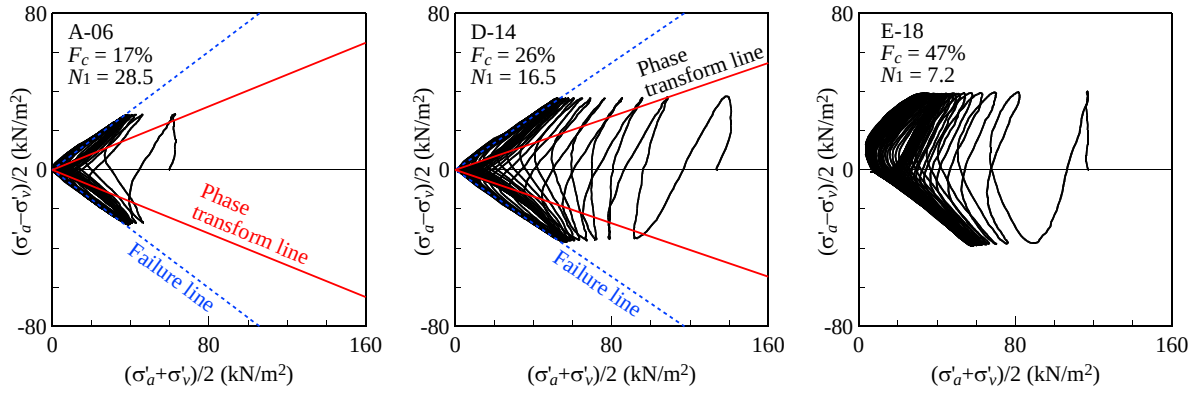

(a) A-06 (F_c = 17 %) (b) D-14 (F_c = 26 %) (c) E-18 (F_c = 47 %)

Fig. 3 Effective stress path diagram of undisturbed soil

5. PROPOSAL OF EMPIRICAL EQUATION

Phase transform angle ϕ_p and internal friction angle ϕ_f are compared as a function of the conversion N value, N_1, in Figs. 4 and 5, respectively. Here, the internal friction angle of the Toyoura sand are evaluated by using the empirical equation by Meyerhof[12].

The undisturbed samples are classified into three categories depending on the fines content, $F_c \leq 20$ %, $20 < F_c \leq 35$ %, and $F_c > 35$ %, respectively and different colors are used in Figs. 4 and 5. The ϕ_p of 28

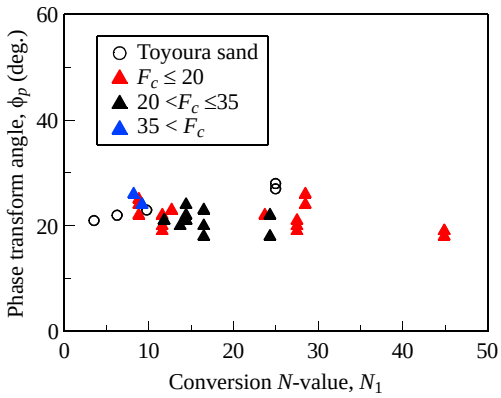

Fig. 4 Phase transform angle vs. N_1

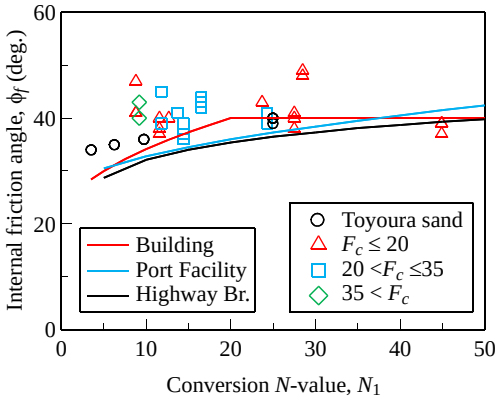

Fig. 5 Internal friction angle vs. N_1

degrees are usually used in FLIP-ROSE, but actual ϕ_p scatters between 18 degreed and 28 degreed as shown in Fig. 4. There is no clear N_1 dependency for the phase transform angle ϕ_p in the undisturbed sands, although that of the Toyoura sand shows that it seems to have N_1 dependency; ϕ_p increases as N_1 increases. Empirical equations for the relationships between ϕ_p and N_1 shown in three typical Japanese design specifications, are also shown in Fig. 5 as solid lines. The test data shows larger values than that in the design specifications in general.

$$\phi_f = 4.8\ln(N_1) + 21 \quad (N > 5) \qquad \text{Highway bridge}^{11)} \tag{2}$$

$$\phi_f = 3.2\left(\frac{100N}{\sigma'_v + 70}\right) + 25 \qquad \text{Port facility}^{13)} \tag{3}$$

$$\left.\begin{aligned} \phi_f &= 20 + \sqrt{20N_1} && (3.5 \leq N_1 \leq 20) \\ \phi_f &= 40 && (20 < N_1) \quad \text{, where } N_1 = N/\sqrt{\sigma'_v/98} \end{aligned}\right\} \qquad \text{Building}^{14)} \tag{4}$$

Relationships between the phase transform angle and the internal friction angle are shown in Fig. 6. Here, the black dashed line is an equation shown in the computer program YUSAYUSA,

$$\tan\phi_p = 0.875\tan\phi_f \tag{5}$$

which is much larger than that of the tests. It is also pointed out that the phase transform angle of the Toyoura sand is generally larger than that of the undisturbed soil, which seems to indicate that excess porewater pressure generation is smaller in the undisturbed soil compared with the Toyoura sand.

It looks that there are strong correlations between the phase transform angles and the internal friction angles in the Toyoura sand and in the undisturbed soil with $F_c \leq 20$ %, but there is no correlation in the undisturbed soil with $F_c > 20$ %. Linear correlations are assumed for these two cases and the coefficients are determined by using the least square method, which results in the following equations. These equations are also shown in Fig. 6.

$$\phi_p = 1.141\phi_f - 17.900 \quad (\text{Toyoura sand, } F_c = 0\ \%) \tag{6}$$

$$\phi_p = 0.543\phi_f - 0.905 \quad \text{(Undisturbed soil, } F_c \le 20\ \%\text{)} \tag{7}$$

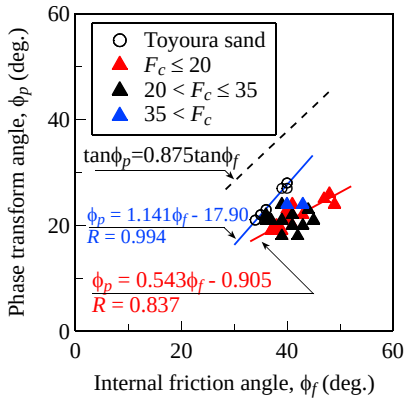

Fig. 6. Internal friction angle vs. phase transform angle

6. CONCLUSIONS

Phase transform angles are evaluated from the liquefaction strength test results for the Toyoura sands and undisturbed soils, and are investigated. The following conclusions are obtained

(1) Phase transform angles lie between 18 and 28 degrees.

(2) There are strong correlations between the phase transform angle and the internal friction angle for the soils with fines content less than 20 %.

(3) Two empirical equations are proposed for these cases; the one is for the Toyoura sand with F_c = 0 % and the other is for the undisturbed soils with $F_c \le 20$ %.

REFERENCES

1) Tatsuoka, F.: Fundamental Study on Deformation Characteristics of Sand by Means of Triaxial Test Apparatus, *Theses submitted to the University of Tokyo*, 1973 (in Japanese).
2) Ishihara, K., Tatsuoka, F. and Yasuda, S.: Undrained Deformation and Liquefaction of Sand under Cyclic Stresses, *Soils and Foundations*, Vol. 15, No. 1, pp. 29–44, 1975.
3) The Japanese Geotechnical Society: *Japanese Standards and Explanations of Laboratory Tests of Geomaterials*, the Japanese Geotechnical Society, Vol. 2, pp. 730–749, 2009 (in Japanese).
4) Yoshida, N. and Towhata, I.: YUSAYUSA-2 and SIMMDL-2, Theory and Practice, 1991; Revised in 2003 (Version 2.1), Tohoku Gakuin University and the University of Tokyo. https://www.kiso.co.jp/yoshida/ (last accessed on October 14, 2020).
5) Morita, T., Iai, S., Liu, H., Ichii, K. and Sato, Y.: Simplified Method to Determine Parameter of FLIP, *Technical Note of the Port and Harbour Research Institute, Ministry of Transport*, No. 803, 1997 (in Japanese).
6) Phase Transform Group, Simplified Parameter Setting WG: *Annual Report of Working in 2017*, FLIP Consortium, pp. 39–40, 2018 (in Japanese).
7) Iai, S., Ueda, K., Tobita, T. and Ozutsumi, O.: Finite Strain Formulation of Strain Space Multiple Mechanism Model for Granular Materials, *International Journal for Numerical and Analytical Methods in Geomechanics*, Vol. 37, pp. 1189–1212, 2013.

8) Iai, S., Tobita, T. and Ozutsumi, O.: Stress Dilatancy Relation in Strain Space Multiple Mechanism Model for Cyclic Behavior of Sand, *Annuals of Disaster Prevention Research Institute, Kyoto University*, No. 51 B, pp. 291–303, 2008 (in Japanese).
9) Mikami, T., Ichii, K., Uemura, K. and Nishina, H.: A Model for Strain Increase of Sand under Cyclic Shear in Undrained Condition, *Japanese Geotechnical Journal*, Vol. 7, No. 1, pp. 311–322, 2012 (in Japanese).
10) The Japanese Geotechnical Society: *Japanese Standards and Explanations of Laboratory Tests of Geomaterials*, the Japanese Geotechnical Society, Vol. 2, pp. 553–569, 2009 (in Japanese).
11) Japan Road Association: *Specifications for Highway Bridges*, Part V, Seismic Design, 2017 (in Japanese).
12) Meyerhof, G. G.: Penetration Tests and Bearing Capacity of Cohesionless Soils, *Journal of the Soil Mechanics and Foundations Division*, American Society of Civil Engineers, Vol. 82, No. SM1, 866, pp. 1–19, 1956.
13) Ports and Harbours Bureau, Ministry of Land, Infrastructure, Transport and Tourism, National Institute for Land and Infrastructure Management, MLIT and Port and Airport Research Institute: *Technical Standards and Commentary of Port and Harbour Facilities in Japan*, the Overseas Coastal Area Development Institute of Japan, Vol. 1, p. 334, 2018 (in Japanese).
14)The Architectural Institute of Japan: *Recommendations for Design of Building Foundations*, 2001 Revision, the Architectural Institute of Japan, p. 114, 2001 (in Japanese).

(Original Japanese Paper Published: October, 2019)
(English Version Submitted: October 15, 2020)
(English Version Accepted: March 10, 2021)